TB, BPN, US, PMB/243662, 9/08/2007

IOP PUBLISHING PHYSICS IN MEDICINE AND BIOLOGY

Phys. Med. Biol. **52** (2007) 1–14 UNCORRECTED PROOF

Derivation of the tumor position from external respiratory surrogates with periodical updating of internal/external correlation

E Kanoulas[1], J A Aslam[1], G C Sharp[2], R I Berbeco[3], S Nishioka[4], H Shirato[5] and S B Jiang[2,6]

[1] College of Computer and Information Science, Northeastern University, Boston, MA, USA
[2] Department of Radiation Oncology, Massachusetts General Hospital and Harvard Medical School, Boston, MA, USA
[3] Department of Radiation Oncology, Brigham and Women's Hospital and Harvard Medical School, Boston, MA, USA
[4] Department of Radiology, NTT Hospital, Sapporo, Japan
[5] Department of Radiation Medicine, Hokkaido University School of Medicine, Sapporo, Japan
[6] Department of Radiation Oncology, University of California San Diego, La Jolla, CA, USA

E-mail: ekanou@ccs.neu.edu

Received 9 February 2007, in final form 2 August 2007
Published DD MMM 2007
Online at stacks.iop.org/PMB/52/1

Abstract

In this work we develop techniques that can derive the tumor position from external respiratory surrogates (abdominal surface motion) through periodically updated internal/external correlation. A simple linear function is used to express the correlation between tumor and surrogate motion. The function parameters are established during a patient setup session with tumor and surrogate positions simultaneously measured at a 30 Hz rate. During treatment, the surrogate position, constantly acquired at 30 Hz, is used to derive the tumor position. Occasionally, a pair of radiographic images is acquired to enable the updating of the linear correlation function. Four update methods, two aggressive and two conservative, are investigated: (A1) shift line through update point; (A2) re-fit line through update point; (C1) re-fit line with extra weight to the update point; (C2) minimize the distances to the update point and previous line fit point. In the present study of eight lung cancer patients, tumor and external surrogate motion demonstrate a high degree of linear correlation which changes dynamically over time. It was found that occasionally updating the correlation function leads to more accurate predictions than using external surrogates alone. In the case of high imaging rates during treatment (greater than 2 Hz) the aggressive update methods (A1 and A2) are more accurate than the conservative ones (C1 and C2). The opposite is observed in the case of low imaging rates.

1. Introduction

Techniques such as beam gating (Kubo and Hill 1996, Kubo and Wang 2000, Kubo *et al* 2000, Minohara *et al* 2000, Ohara *et al* 1989, Ramsey *et al* 1999a, 1999b, Shimizu *et al* 2000, 2001, Shirato *et al* 1999, 2000, 2001, 2003, Vedam *et al* 2001, Keall *et al* 2001, 2002, 2005, Harada *et al* 2002, Jiang 2006a, 2006b) or beam tracking (Murphy 2002, 2004, Murphy *et al* 2003, Adler *et al* 1999, Schweikard *et al* 2000, Neicu *et al* 2003, Papiez 2003, Rangaraj and Papiez 2005, Papiez and Rangaraj 2005, Wijesooriya *et al* 2005, Webb 2005a, 2005b, Neicu *et al* 2006) hold promise to reduce the incidence and severity of normal tissue complications and to increase local control through dose escalation for mobile tumors in the thorax and abdomen. Precise target localization in real time is particularly important in such techniques due to the reduced clinical tumor volume to planning target volume (CTV-to-PTV) margin and/or escalated dose. Direct localization of the tumor mass in real time is difficult, if not impossible (Berbeco *et al* 2005a). Instead, various surrogates are used to derive the tumor position during the treatment, including implanted fiducial markers and markers placed on the surface of the patient's abdomen.

The weakness of using external surrogates alone may be the lack of accuracy due to the uncertainty in the correlation between the external surrogates and internal tumor position (Ionascu *et al* 2006, Hoisak *et al* 2004). The precision of tumor localization is often satisfactory with implanted fiducial markers inside or near the tumor. However, fluoroscopically tracking the markers requires a radiation dose for imaging. For standard fractionated treatments the imaging dose can be more than what is clinically acceptable.

When only the internal tumor position is tracked, the imaging frequency can be reduced by predicting future tumor positions (Murphy 2004, Vedam *et al* 2004), e.g. by using predictive filters (Sharp *et al* 2004), nonlinear neural networks (Murphy and Dieterich 2006) or modeling the tumor motion with piece-wise linear approximations (Wu *et al* 2004). The combination of internal marker position with external surrogate signal can further reduce the imaging rate (Schweikard *et al* 2000, Murphy 2004, Isaksson *et al* 2005, Nuyttens *et al* 2006, Casamassima *et al* 2006). The external surrogates are constantly tracked and used to derive the tumor position. Once in a while the internal marker position is acquired and used to re-calibrate the correlation between internal tumor and external surrogate motion (Seppenwoolde *et al* 2006).

Seppenwoolde *et al* (2007) investigate the accuracy of tumor derivation from an external surrogate by employing a linear and a plynomial model to capture the relationship between tumor and external surrogate position. During the patient setup session both model parameters are estimated by fitting a small number of tumor/external surrogate positions into the models. The final selection of which model will be used during treatment is based on the comparison of a modified form of the models fitting error. During treatment, once a new radiographic image of the tumor is acquired, the new data along with the data used in the previous fitting are fitted again to recalibrate the model parameters. (This is done in a sliding window mode, where the first acquired point used in the previous fitting is replaced by the most recently acquired one.)

In this work, we derive the tumor position from external surrogates through the calibrated external/internal correlation before each fraction of treatment. We express the relation between internal tumor and external surrogate position with a simple linear model. The correlation is updated during the treatment periodically by acquiring radiographic images of the internal marker or tumor position. Aggressive and conservative update methods are investigated. This way, the imaging frequency, thus the imaging dose, can be greatly reduced to a clinically acceptable level and the target localization accuracy can be greatly improved compared to using external surrogates alone.

Table 1. Information about the patients studied. Patient 5 was treated twice, at the same site, with two months difference. The tumor site is indicated using the common anatomical notation for lung segmentation, i.e, S1-3 is the upper lobe, S4-5 is the middle lobe and S6-10 is the lower lobe.

Patient	Age	Gender	Tumor pathology	Number of bbs	Tumor site	Prescribed dose (Gy)	Fraction
1	47	F	Adenocarcinoma	4	Rt. S7	N/A	1
2	70	F	Adenocarcinoma	3	Lt. S6	N/A	1
3	71	F	Adenocarcinoma	2	Rt. S5	N/A	1
4	47	F	Adenocarcinoma	3	Rt. S4	48	8
5	81	M	Squamous cell carcinoma	3	Rt. S2b	48	4
5						40	8
6	61	M	Small cell lung carcinoma	3	Rt. S10	40	8
7	68	M	Squamous cell carcinoma	3	Rt. S6	48	4
8	85	M	Adenocarcinoma	3	Rt. S8	48	4

Table 2. Information about the mean and standard deviation of pick to pick tumor motion over all fractions of treatment for each patient in the LR, SI and AP directions measured in mm.

	LR motion		SI motion		AP motion	
Patient	Avg	Std	Avg	Std	Avg	Std
1	4	0	24	2	10	1
2	4	0	15	0	5	0
3	7	0	10	0	11	0
4	2	0	10	0	8	0
5	3	1	12	1	6	1
6	2	0	17	3	1	0
7	2	0	13	1	2	0
8	4	0	26	3	8	1

2. Methods and materials

2.1. Patient data

A total of eight lung patients with implanted fiducial markers were studied. The data used for the study were collected at the NTT Hospital in Sapporo, Japan Berbeco *et al* (2005b). Details for each patient are given in table 1. Patients 1–3 did not receive treatment. The data were acquired for organ motion study in a single fraction. Patient 5 was treated twice, two months apart. This study includes patients with superior–inferior (SI) tumor motion greater than 1 cm peak to peak. The amplitude of the tumor motion in the other two directions, right–left (RL) and anterior–posterior (AP), is of a comparatively smaller range in most cases with the exception of one patient where the tumor motion in all directions is close to 1 cm. The mean motion from pick to pick over all fractions of treatment and its standard deviation for each patient in the LR, SI and AP directions are given in table 2.

Synchronized internal marker positions and external abdominal surface positions were measured during the entire course of treatment at a 30 Hz frequency. Therefore, the log files contain a three-dimensional (3D) tumor position and a one-dimensional external surface position at every $1/30$ of a second.

A Mitsubishi real-time radiation therapy (RTRT) system (Shirato *et al* 2000) was used to track the 3D tumor position. Patients with abdominal and thoracic tumors, treated with this

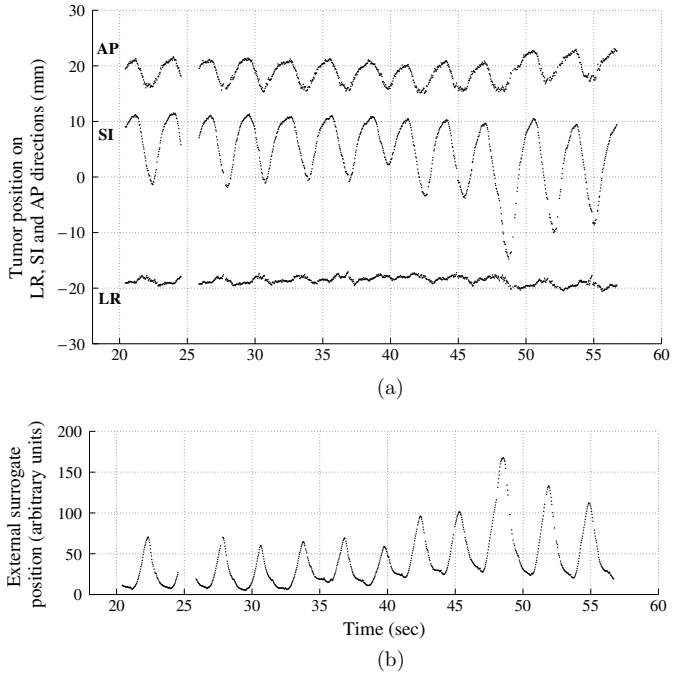

Figure 1. Tumor and external surrogate position for patient 8. (a) The tumor in LR, SI and AP directions tracked by the RTRT system for patient 8. (b) The external surrogate monitored by the AZ-733V system for patient 8.

system, typically have two to four 1.5 mm diameter gold ball bearings (bbs) implanted in or near the tumor Shirato *et al* (2003). These markers are tracked in real time with diagnostic x-ray flouroscopy. The data output of this system for patient 8 can be seen in figure 1(a).

An AZ-733V external respiratory gating system (Anzai Medical, Tokyo, Japan), installed and integrated with the RTRT system, was used to monitor the movement of the patient's abdominal surface. A laser attached to the treatment couch and placed orthogonal to the patient's skin surface was used. The abdomen motion is tracked by measuring the relative position of the laser reflected light. The data output of this system for patient 8 can be seen in figure 1(b).

2.2. Correlation function between tumor and external surrogate motion

A linear function is used to express the correlation between internal tumor and external surrogate position. To justify this choice the Pearson's correlation coefficient, ρ, between the tumor and external surrogate position was calculated and *t*-tests were used to assess its significance.

The absolute value of the correlation coefficient computed for the SI direction varied from 0.8801 to 0.9891, verifying a significant degree of linear correlation between the tumor position in this direction and the external surrogate (1 and -1 are the maximum and minimum values that ρ can obtain and express a perfect positive and perfect negative linear correlation, respectively). The correlation coefficient varies in a larger range in the case of the LR and AP directions with mean absolute values of 0.6167 and 0.5862, respectively. A cross-correlation

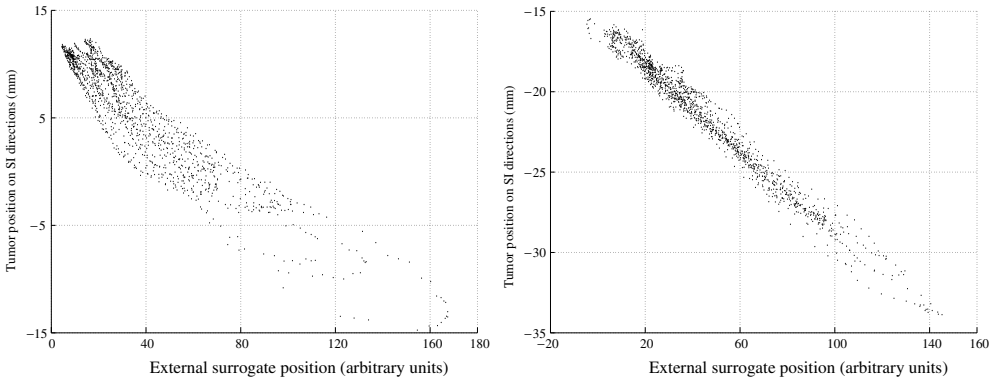

(a) Patient 8 (b) Patient 4

Figure 2. External surrogate position versus tumor position in the SI direction.

analysis in these two direction reveals that tumor and external surrogate motion demonstrate a phase difference that significantly accounts for the low mean values of the correlation coefficient.

In the rest of this work we only focus in the SI direction of tumor motion mainly because of the significance of the tumor motion in this direction.

In figure 2 tumor positions in the SI direction are scattered against the surrogate positions for patients 8 and 4 for a single fraction of treatment. The shape of the scattered values can indicate, to some extent, the characteristics of the correlation function. Changes in the slope, the offset from the origin and the width of the elliptical shapes geometrically illustrate scale, shift and phase differences between the SI tumor motion and the surrogate motion even within each breathing cycle. The correlation function should be able to account for such differences. For the purpose of this work a simple linear function is selected to express the observed correlation. Therefore, $\hat{y}_t = a \cdot e_t + b$, where $\hat{y}_t$ and e_t are the predicted SI tumor position and the surrogate position, respectively. The model parameters a and b express the scale and the shift difference between the external surrogate and the tumor motion, respectively.

During the patient setup session, both tumor and surrogate positions are acquired at a rate of 30 Hz for a few breathing cycles. The parameters a and b are estimated by fitting the linear function to the data obtained during this session. That is, the values of the parameters a and b are selected such that the squared error between the real tumor position in the SI direction y_t and the estimated value given by the linear model, $a \cdot e_t + b$, is minimized (figure 3). During treatment, the tumor position is estimated based on the external surrogate position, still acquired at a 30 Hz rate, and the established linear function obtained during the setup session (figure 4).

In the rest of the work (figures 3–8) the dataset from the first fraction of treatment for patient 8 is used to illustrate our results.

2.3. Update methods for correlation function

Usually, the current practice of external gating or tracking implies that no tumor position is acquired during the treatment (Jiang 2006a). Tumor localization is performed based on the correlation function established during the patient setup session and the external surrogate positions monitored during treatment. Under the assumption of stationary correlation (i.e., the

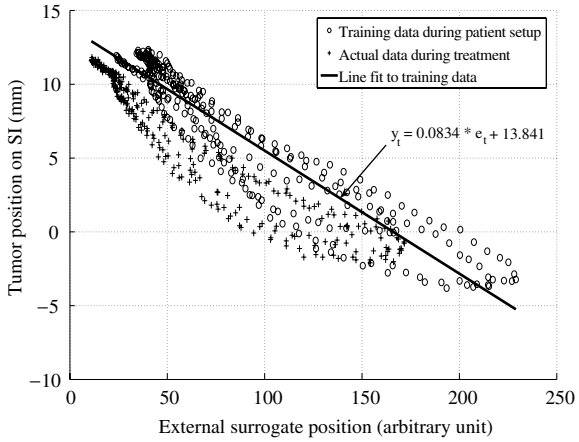

Figure 3. External surrogate position versus tumor position in the SI direction during patient setup and treatment sessions. The line that best fits the training data along with the constantly obtained external surrogate positions is used to predict the tumor position during treatment.

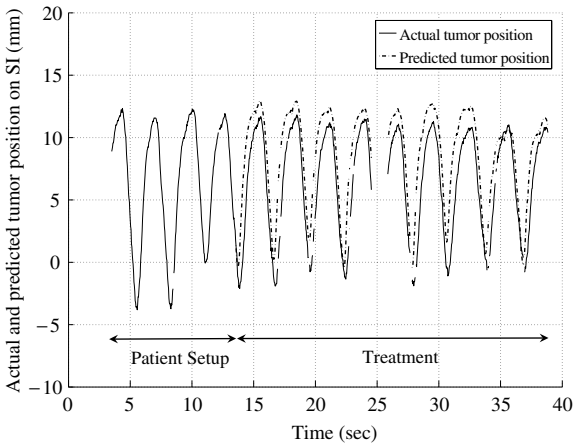

Figure 4. Actual and predicted tumor position in the SI direction. After the first breathing cycle of the treatment session, there is a constant shifting between the predicted and the actual tumor position indicating a change of the correlation between tumor and surrogate motion.

correlation function between tumor position and external surrogate position does not change with the time), the prediction accuracy merely depends on the goodness of the function fit.

However, as one can notice in figure 3, most of the data points (tumor position versus external surrogate position) during treatment (denoted by plus signs) are located to the left of the obtained line, indicating a change in the relation between tumor and external surrogate motion. This can be further suggested by observing figure 4, where tumor position is constantly overestimated by the obtained model.

This indicates a dynamically varying correlation between external surrogate and tumor motion. In this case, the correlation function parameters, a and b, need to be periodically updated. Acquiring radiographic images during treatment at a low frequency, such as 1 image every 10 s (0.1 Hz), so update points (tumor versus surrogate position) can be obtained, may be enough to update the correlation function.

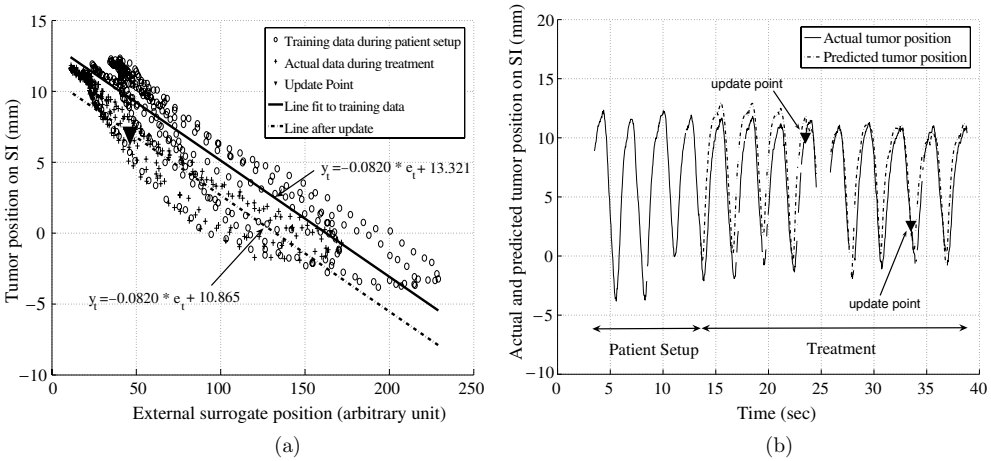

Figure 5. (A1) Shift the line through the update point. (a) External surrogate position versus tumor position on SI during patient setup and treatment sessions. (b) Actual and predicted tumor position in the SI direction.

Upon the observation of an update point, (e_{now}, y_{now}), different update methods to calibrate the correlation function parameters have been explored. Intuitively, when an update point deviates from the obtained line, it can either be a regular error due to the over-determined system of tumor–external surrogate points that the line does not solve exactly (e.g. as most of the training data, denoted by circles in figure 3) or indicate that there is a change in the correlation function. With respect to our belief regarding the deviation of update point from the line, we explore two aggressive and two conservative update methods. The aggressive ones are based on the belief that the update point indicates a change on the correlation function. The conservative ones try to compensate for both cases and balance between the previous knowledge about the correlation function (expressed by the tumor–external surrogate points during the patient setup or by the obtained line) and the new knowledge expressed by the newly acquired tumor–external surrogate point.

In particular, we explore the following update methods:

(A1) *Shift line through update point.* The line is shifted to pass through (e_{now}, y_{now}), i.e., b is the only parameter updated. Shift update accounts only for changes in the mean position of either the tumor or the external surrogate motion or both of them. The method aggressively corrects the correlation function, readjusting it according to the recently acquired tumor–external surrogate point.

The updating method is illustrated in figure 5. In figure 5(a) the solid line is the correlation function acquired by fitting the training data during patient setup. The triangle denotes the update point obtained 10 s after the start of the treatment. The dashed line is the correlation function obtained after the first update. Figure 5(b) demonstrates the predicted tumor positions compared to the actual tumor position in the SI direction. The triangles denote the tumor positions acquired during treatment (0.1 Hz). As one can observe, after each update the correlation function is corrected and the prediction quality substantially improves.

(A2) *Re-fit line and force it through the update point.* The linear function is fitted to both training data (i.e., data gathered during the patient setup session) and data acquired

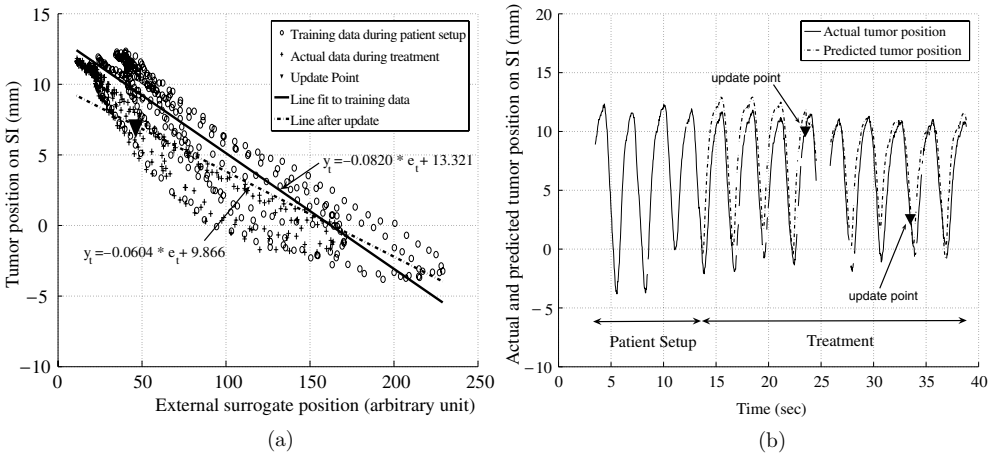

(a) (b)

Figure 6. (A2) Re-fit the line and force it through the update point. (a) External surrogate position versus tumor position on SI during patient setup and treatment sessions. (b) Actual and predicted tumor position in the SI direction.

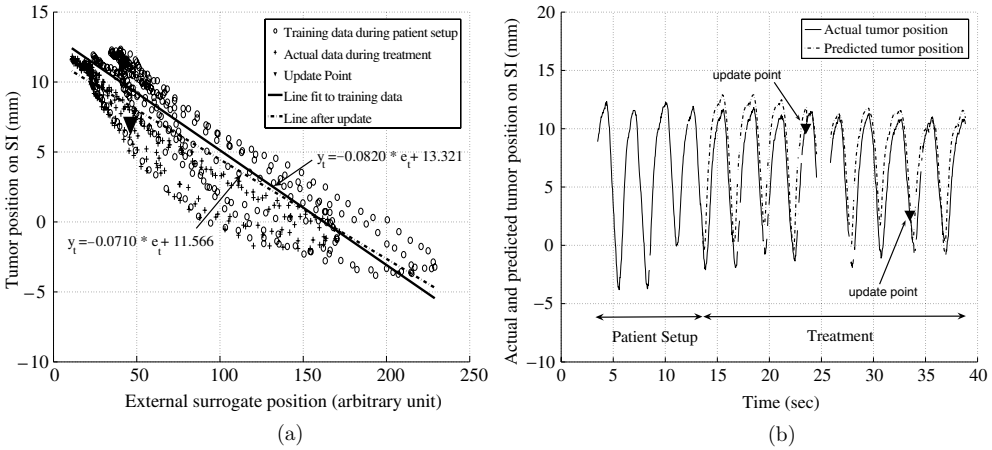

(a) (b)

Figure 7. (C1) Re-fit the line with extra weight to the update point. (a) External surrogate position versus tumor position on SI during patient setup and treatment sessions. (b) Actual and predicted tumor position in the SI direction.

during the treatment session under the constraint that the obtained line after the update passes through the update point, $(e_{\text{now}}, y_{\text{now}})$ (figure 6). The method is still aggressive but in contrast to the previous method, it can compensate for both shift and scale changes in the motions relation.

(C1) *Re-fit line with extra weight to update point.* The linear function is fitted to training data and data acquired during treatment session. Within the fitting process, $(e_{\text{now}}, y_{\text{now}})$ is given a larger weight than the rest of the data. In this way, previously obtained information regarding the correlation function is combined with information given by the recently acquired point. Therefore, the method moderately update the correlation function towards $(e_{\text{now}}, y_{\text{now}})$.

The method is illustrated in figure 7.

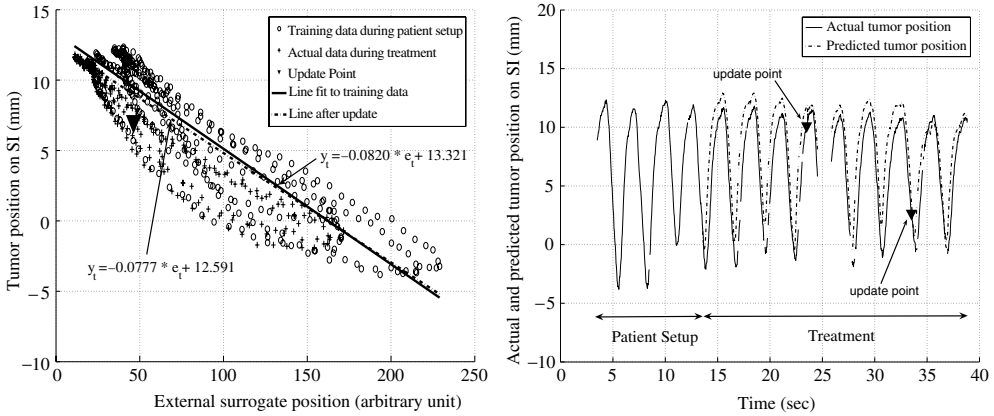

Figure 8. (C2) Minimize the distance to the previous line and the update point. (a) External surrogate position versus tumor position on SI during patient setup and treatment sessions. (b) Actual and predicted tumor position in the SI direction.

(C2) *Minimize distance to previous line and update point.* Similarly to the previous method, this last method tries to balance between the need to be conservative, i.e., to keep the new model parameters close to the previous ones, and corrective, thus to reduce the prediction error of new model parameters upon a future observation of $(e_{\text{now}}, y_{\text{now}})$.

Let $f_{a,b}(e_t) = a \cdot e_t + b$, and $f_{a',b'}(e_t) = a' \cdot e_t + b'$, where a and b are the old function parameters while a' and b' are the ones we want to compute. Under this setup, the two extremes we could follow in order to update the model parameters would be (a) $a' = a$ and $b' = b$ (conservative) and (b) a' and b' are those parameters for which $y_{\text{now}} = a' \cdot e_{\text{now}} + b'$ (aggressive).

A better idea would be to balance between the two approaches by minimizing $\| f_{a,b} - f_{a',b'} \| + \eta \cdot (y_{\text{now}} - a' \cdot e_{\text{now}} + b')^2$. $\| f_{a,b} - f_{a',b'} \|$ denotes some distance function between the two line. In our case we use $\| f_{a,b} - f_{a',b'} \| = (\int_{\alpha}^{\beta} (f_{a,b}(e) - f_{a',b'}(e))^p de)^{1/p}$, with $e \in [\alpha, \beta]$. The surrogate motion range (i.e., α and β) can be approximated by the motion range during the patient setup session. For $p = 2$ the distance function is the well-known Euclidean (L2) distance between the two lines. The parameter η dictates how much conservative we are in our updates.

Similarly to figure 7, in figure 8 one can observe the dashed line to balance between the update point (triangle) and the previously acquired line (solid line).

3. Results

In the study performed eight lung patients over several days and treatment fractions were studied. Among all datasets collected, only those at which the tumor motion is significant were used (85 out of 180 datasets). In particular, in all considered datasets, the tumor motion from peak to peak varied between 10 and 37 mm, with an average range of 17.2 mm and a standard deviation 6.5 mm.

The patient setup session lasts approximately three to four breathing cycles (11 s) during which the linear model is trained. We tested all four update methods for different update frequencies varying from 15 Hz to 0.05 Hz (that is varying from 1 image every 0.066 s to 1

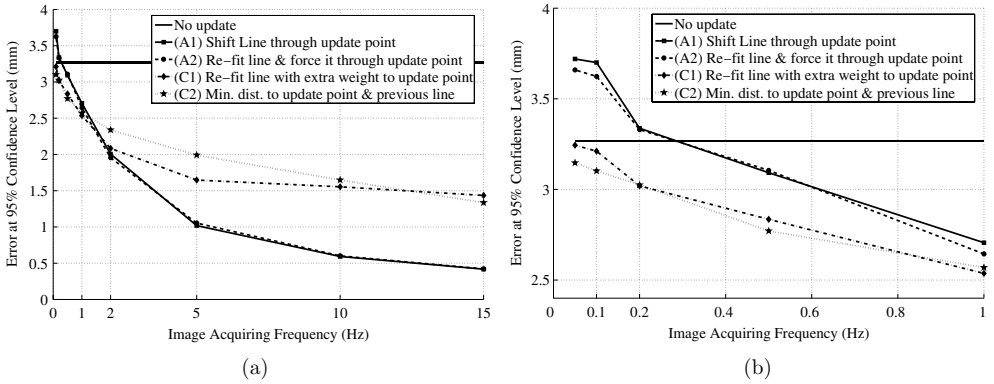

Figure 9. Tumor motion in the SI direction: the absolute prediction error at a 95% confidence level for all four update methods along with the case of no updates for different update frequencies. Figure (b) is a duplicate of figure (a) magnified at frequencies lower than 2 Hz.

image every 20 s). In this study we noticed that the quality of the prediction during treatment highly depends on the breathing phase at which the tumor position is acquired for updating. In particular, updating the linear model during the end of exhale results in better predictions compared to any other breathing phase. To cancel this effect and isolate the effects of different methods for different update frequencies on the quality of the predictions we repeated the experiments several times by forcing a random delay varying from 0 to 3 s (approximately the duration of one breathing cycle) between the end of the patient setup session and the beginning of the treatment. In this way we randomize the breathing phase during which the radiographic image is acquired. As an alternative to the aforementioned methodology, one can conduct the experiments in a randomized manner. Let f be the frequency at which we would like to acquire radiographic images and $f_{\max}$, the maximum frequency at which radiographic images could possibly be obtained (in the case of this current study $f_{\max}$ is 30 Hz). Instead of acquiring the radiographic images at a constant rate f, we perform the following random experiment every $1/f_{\max}$ seconds. We toss a coin and with probability equal to $f/f_{\max}$ we decide to obtain a radiographic image. In this fashion the expected imaging frequency is f while the breathing phase during which we acquire this image is random. (The results of this alternative method are identical to those of the former method and therefore they are not reported.)

During treatment the tumor position in the SI direction is predicted using the linear model and the predicted values are compared with the actual tumor position. The absolute error at 95% confidence level is reported. More specifically, a value cl is reported for combinations of update method and update frequency such that 95% of the absolute prediction error is less than cl.

The results of the study are illustrated in figure 9. The mean over all patients upper bound for 95% of the absolute error between predicted and actual tumor position in the SI direction for all four update methods along with the case of external tracking (i.e., no updates during the treatment) and for different radiographic image acquiring frequencies is depicted in figure 9(a). Figure 9(b) illustrates the same results as (a) with a focus on frequencies less that 2 Hz.

Note that for frequencies higher than 2 Hz aggressive methods result in lower prediction error than conservative methods, while the opposite is true for frequencies lower than 2 Hz.

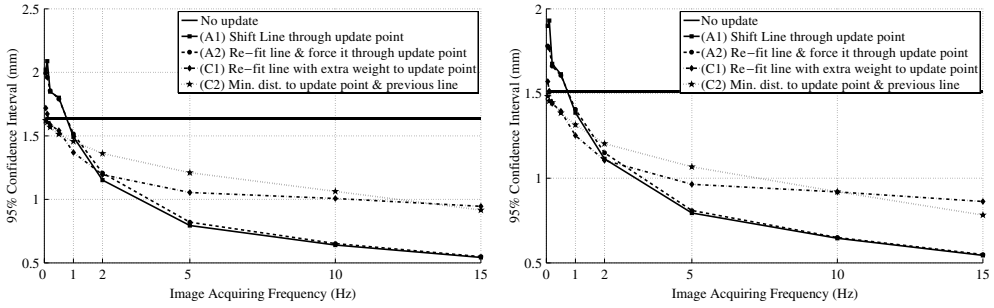

Figure 10. Tumor motion in the AP direction : The absolute prediction error at a 95% confidence level for all four update methods along with the case of no updates for different update frequencies. (a) A linear function between the current tumor position and the current surrogate position is used. (b) A linear function between the current tumor position and past surrogate position is used.

When the imaging rate is low, the number of update points obtained does not suffice to accurately characterize the changes of the correlation function. The deviation of the update point from the line may simply be a regular error of the fitting process. This explains the reason why the methods that balance their belief between previously obtained information and the update point demonstrate better results. In contrast, when the imaging rate is high, update points can better qualify changes in correlation. In this case, larger belief on the update points results in high accuracy of predictions and therefore updating aggressively appears to be a better strategy.

4. Conclusions and discussion

External surrogate and tumor motion are highly correlated. We used a linear function between tumor and external surrogate position to express their correlation. Yet the correlation changes with the time leading to large error in prediction if only the external surrogate is used to predict the tumor position during treatment. Coping with non-stationary correlation requires periodical update of the correlation function.

In this work we investigated the employment of two aggressive and two conservative updating methods for different update frequencies. In most cases, updating the correlation function significantly improved the quality of predictions. The aggressive methods lead to better results when the updating frequency was high (15 Hz down to 2 Hz) while for low frequencies (2 Hz down to 0.05 Hz) conservative methods appeared to be more appropriate.

In the current work we focused and reported our findings in the SI direction of the tumor motion due to the significance of the motion in that direction (10–37 mm). However, we have studied and conducted experiments for the tumor motion in the AP direction as well (the motion in LR direction is minimal). Figure 10 depicts the results of this study. The mean over all patients upper bound for 95% of the absolute error between predicted and actual tumor position in AP direction for all four update methods along with the case of external tracking (i.e., no updates during the treatment) and for different radiographic image acquiring frequencies is reported. Figure 10(a) illustrates these results with a linear function between the current tumor position in AP and the current surrogate position being employed.

Furthermore, we applied a phase shift in the linear model and found that for the SI direction there is no improvement while for the AP motion there is improvement. This is due to the fact that there is a constant phase shift between tumor motion in AP direction and external surrogate motion. However, for SI direction, the phase shift varies within the fraction. Figure 10(b) illustrates the results with a phase shift applied in the linear function.

Moreover, in the future we plan to study the employment of more complex linear functions (e.g. functions that include current and past positions) and the utilization of transfer functions.

Furthermore, in the current work we only explore updating methods of constant imaging frequency during treatment. In the future we plan to investigate adaptive updating methods where imaging is in control of the algorithm. Preliminary work in this direction shows promising results (better updates and lower imaging frequency).

In the case of adaptive updating methods there is a number of important questions that arise and which we plan to further explore. For instance, does a change (base line shift, amplitude change, etc) of the surrogate motion indicate any change in the relationship between the tumor and external surrogate? If such a question can be answered deterministically then an algorithm would always know when the relationship between tumor and surrogate motion changes and therefore needs recalibration. Another significant question to be answered is whether or not the quality of predictions depends on the breathing phase at which the update images are acquired. Preliminary results show that updating during the end of exhale is able to detect and correct significant changes in the tumor/surrogate relationship.

Acknowledgments

This material is based upon work supported by the National Science Foundation under grant no IIS-0533625 and grant no CCF-0418390. Any opinions, findings, and conclusions or recommendations expressed in this material are those of the author(s) and do not necessarily reflect the views of the National Science Foundation.

References

Adler J R, Murphy M J, Chang S D and Hancock S L 1999 Image-guided robotic radiosurgery *Neurosurgery* **44** 1299–306 (discussion 1306–7)

Berbeco R I, Mostafavi H, Sharp G C and Jiang S B 2005a Towards fluoroscopic respiratory gating for lung tumours without radiopaque markers *Phys. Med. Biol.* **50** 4481–90

Berbeco R I, Nishioka S, Shirato H, Chen G T Y and Jiang S B 2005b Residual motion of lung tumours in gated radiotherapy with external respiratory surrogates *Phys. Med. Biol.* **50** 3655–67

Casamassima F, Cavedon C, Francescon P, Stancanello J, Avanzo M, Cora S and Scalchi P 2006 Use of motion tracking in stereotactic body radiotherapy: evaluation of uncertainty in off-target dose distribution and optimization strategies *Acta Oncol.* **45** 943–7

Harada T, Shirato H, Ogura S, Oizumi S, Yamazaki K, Shimizu S, Onimaru R, Miyasaka K, Nishimura M and Dosaka-Akita H 2002 Real-time tumor-tracking radiation therapy for lung carcinoma by the aid of insertion of a gold marker using bronchofiberscopy *Cancer* **95** 1720–7

Hoisak J D P, Sixel K E, Tirona R, Cheung P C F and Pignol J 2004 Correlation of lung tumor motion with external surrogate indicators of respiration *Int. J. Radiat. Oncol. Biol. Phys.* **60** 1298–306

Ionascu D, Jiang S B, Nishioka S, Longberg F, Shirato H and Berbeco R I 2006 Mo-d-valb-04: internal–external correlation investigations of respiratory induced motion of lung tumors *Med. Phys.* **33** 2161

Isaksson M, Jalden J and Murphy M J 2005 On using an adaptive neural network to predict lung tumor motion during respiration for radiotherapy applications *Med. Phys.* **32** 3801–9

Jiang S B 2006a Technical aspects of image-guided respiration-gated radiation therapy *Med. Dosim.* **31** 141–51

Jiang S B 2006b Radiotherapy of mobile tumors *Semin. Radiat. Oncol.* **16** 239–48

Keall P J, Joshi S, Vedam S S, Siebers J V, Kini V R and Mohan R 2005 Four-dimensional radiotherapy planning for dmlc-based respiratory motion tracking *Med. Phys.* **32** 942–51

Keall P J, Kini V R, Vedam S S and Mohan R 2001 Motion adaptive x-ray therapy: a feasibility study *Phys. Med. Biol.* **46** 1–10

Keall P J, Kini V R, Vedam S S and Mohan R 2002 Potential radiotherapy improvements with respiratory gating *Australas. Phys. Eng. Sci. Med.* **25** 1–6

Kubo H D and Hill B C 1996 Respiration gated radiotherapy treatment: a technical study *Phys. Med. Biol.* **41** 83–91

Kubo H D, Len P M, Minohara S and Mostafavi H 2000 Breathing-synchronized radiotherapy program at the University of California Davis Cancer Center *Med. Phys.* **27** 346–53

Kubo H D and Wang L 2000 Compatibility of varian 2100c gated operations with enhanced dynamic wedge and imrt dose delivery *Med. Phys.* **27** 1732–8

Minohara S, Kanai T, Endo M, Noda K and Kanazawa M 2000 Respiratory gated irradiation system for heavy-ion radiotherapy *Int. J. Radiat. Oncol. Biol. Phys.* **47** 1097–103

Murphy M J 2002 Fiducial-based targeting accuracy for external-beam radiotherapy *Med. Phys.* **29** 334–44

Murphy M J 2004 Tracking moving organs in real time *Semin. Radiat. Oncol.* **14** 91–100

Murphy M J, Chang S D, Gibbs I C, Le Q T, Hai J, Kim D, Martin D P and Adler J R Jr 2003 Patterns of patient movement during frameless image-guided radiosurgery *Int. J. Radiat. Oncol. Biol. Phys.* **55** 1400–8

Murphy M J and Dieterich S 2006 Comparative performance of linear and nonlinear neural networks to predict irregular breathing *Phys. Med. Biol.* **51** 5903–14

Neicu T, Berbeco R, Wolfgang J and Jiang S B 2006 Synchronized moving aperture radiation therapy (smart): improvement of breathing pattern reproducibility using respiratory coaching *Phys. Med. Biol.* **51** 617–36

Neicu T, Shirato H, Seppenwoolde Y and Jiang S B 2003 Synchronized moving aperture radiation therapy (smart): average tumour trajectory for lung patients *Phys. Med. Biol.* **48** 587–98

Nuyttens J J, Prevost J B, Praag J, Hoogeman M, van Klaveren R J, Levendag P C and Pattynama P M T 2006 Lung tumor tracking during stereotactic radiotherapy treatment with cyberknife: marker placement and early results *Acta Oncol.* **45** 961–5

Ohara K, Okumura T, Akisada M, Inada T, Mori T, Yokota H and Calaguas M J 1989 Irradiation synchronized with respiration gate. *Int. J. Radiat. Oncol. Biol. Phys.* **17** 853–7

Papiez L 2003 The leaf sweep algorithm for an immobile and moving target as an optimal control problem in radiotherapy delivery *Math. Comput. Model.* **37** 735–45

Papiez L and Rangaraj D 2005 Dmlc leaf-pair optimal control for mobile deforming target *Med. Phys.* **32** 275–85

Ramsey C R, Cordrey I L and Oliver A L 1999a A comparison of beam characteristics for gated and nongated clinical x-ray beams *Med. Phys.* **26** 2086–91

Ramsey C R, Scaperoth D, Arwood D and Oliver A L 1999b Clinical efficacy of respiratory gated conformal radiation therapy *Med. Dosim.* **24** 115–9

Rangaraj D and Papiez L 2005 Synchronized delivery of dmlc intensity modulated radiation therapy for stationary and moving targets *Med. Phys.* **32** 1802–17

Schweikard A, Glosser G, Bodduluri M, Murphy M J and Adler J R 2000 Robotic motion compensation for respiratory movement during radiosurgery *Comput. Aided Surg.* **5** 263–77

Seppenwoolde Y, Berbeco R I, Nishioka S, Shirato H and Heijmen B 2007 Accuracy of tumour motion compensation algorithm from a robotic respiratory tracking system: a simulation study *Med. Phys.* **34** 2774–84

Seppenwoolde Y, Nishioka S, Shirato H and Heijmen B 2006 Accuracy of tumour tracking to compensate respiratory motion, assessed with continuously recorded internal and external markers *American Society for Therapeutic Radiology and Oncology (ASTRO): 49th Annual Meeting* pp 42–3

Sharp G C, Jiang S B, Shimizu S and Shirato H 2004 Prediction of respiratory tumour motion for real-time image-guided radiotherapy *Phys. Med. Biol.* **49** 425–40

Shimizu S, Shirato H, Kitamura K, Shinohara N, Harabayashi T, Tsukamoto T, Koyanagi T and Miyasaka K 2000 Use of an implanted marker and real-time tracking of the marker for the positioning of prostate and bladder cancers *Int. J. Radiat. Oncol. Biol. Phys.* **48** 1591–7

Shimizu S, Shiratoand H, Ogura S, Akita-Dosaka H, Kitamura K, Nishioka T, Kagei K, Nishimura M and Miyasaka K 2001 Detection of lung tumor movement in real-time tumor-tracking radiotherapy *Int. J. Radiat. Oncol. Biol. Phys.* **51** 304–10

Shirato H *et al* 2000 Four-dimensional treatment planning and fluoroscopic real-time tumor tracking radiotherapy for moving tumor *Int. J. Radiat. Oncol. Biol. Phys.* **48** 435–42

Shirato H *et al* 2001 Physical aspects of a real-time tumor-tracking system for gated radiotherapy *Int. J. Radiat. Oncol. Biol. Phys.* **51** 304–10

Shirato H *et al* 2003 Feasibility of insertion/implantation of 2.0-mm-diameter gold internal fiducial markers for precise setup and real-time tumor tracking in radiotherapy *Int. J. Radiat. Oncol. Biol. Phys.* **56** 240–7

Shirato H, Shimizu S, Shimizu T, Nishioka T and Miyasaka K 1999 Real-time tumour-tracking radiotherapy *Lancet* **353** 1331–2

Vedam S S, Keall P J, Docef A, Todor D A, Kini V R and Mohan R 2004 Predicting respiratory motion for four-dimensional radiotherapy *Med. Phys.* **31** 2274–83

Vedam S S, Keall P J, Kini V R and Mohan R 2001 Determining parameters for respiration-gated radiotherapy *Med. Phys.* **28** 2139–46

Webb S 2005a The effect on imrt conformality of elastic tissue movement and a practical suggestion for movement compensation via the modified dynamic multileaf collimator (dmlc) technique *Phys. Med. Biol.* **50** 1163–90

Webb S 2005b Limitations of a simple technique for movement compensation via movement-modified fluence profiles *Phys. Med. Biol.* **50** N155–61

Wijesooriya K, Bartee C, Siebers J V, Vedam S S and Keall P J 2005 Determination of maximum leaf velocity and acceleration of a dynamic multileaf collimator: implications for 4d radiotherapy *Med. Phys.* **32** 932–41

Wu H, Sharp G C, Salzberg B, Kaeli D, Shirato H and Jiang S B 2004 A finite state model for respiratory motion analysis in image guided radiation therapy *Phys. Med. Biol.* **49** 5357–72